Molecular Dynamics Study of Substance P Peptides Partitioned in a Sodium Dodecylsulfate Micelle

Troy Wymore and Tuck C. Wong
Department of Chemistry, University of Missouri, Columbia, Missouri 65211 USA

ABSTRACT Two neuropeptides, substance P (SP) and SP-tyrosine-8 (SP-Y8), have been studied by molecular dynamics (MD) simulation in an explicit sodium dodecylsulfate (SDS) micelle. Initially, distance restraints derived from NMR nuclear Overhauser enhancements (NOE) were incorporated in the restrained MD (RMD) during the equilibration stage of the simulation. It was shown that when SP-Y8 was initially placed in an insertion (perpendicular) configuration, the peptide equilibrated to a surface-bound (parallel) configuration in ~450 ps. After equilibration, the conformation and orientation of the peptides, the solvation of both the backbone and the side chain of the residues, hydrogen bonding, and the dynamics of the peptides were analyzed from trajectories obtained from the RMD or the subsequent free MD (where the NOE restraints were removed). These analyses showed that the peptide backbones of all residues are either solvated by water or are hydrogen-bonded. This is seen to be an important factor against the insertion mode of interaction. Most of the interactions come from the hydrophobic interaction between the side chains of Lys-3, Pro-4, Phe-7, Phe-8, Leu-10, and Met-11 for SP, from Lys-3, Phe-7, Leu-10, and Met-11 in SP-Y8, and the micellar interior. Significant interactions, electrostatic and hydrogen bonding, between the N-terminal residues, Arg-Pro-Lys, and the micellar headgroups were observed. These latter interactions served to affect both the structure and, especially, the flexibility, of the N-terminus. The results from simulation of the same peptides in a water/CCl_4 biphasic cell were compared with the results of the present study, and the validity of using the biphasic system as an approximation for peptide-micelle or peptide-bilayer systems is discussed.

INTRODUCTION

Peptide-membrane interactions play important roles in many biological processes (Schwyzer, 1992; White and Wimley, 1994), and have been the subject of studies by many experimental and computational techniques. When liquid-state (or high resolution) NMR techniques are used for investigating peptide-membrane interactions, micelles have often been used as mimics of the membrane environment (Opella, 1997). Micelles mimic the membrane environment by forming spherical aggregates where the hydrophobic tails are located in the core with the polar headgroup on the surface (Gennis, 1989). Since micelles have a short rotational correlation time (in nanoseconds), they are appropriate for high resolution liquid-state NMR studies where other membrane mimics are inappropriate because of their anisotropic nature or size (Soderman et al., 1988). Micelles have been shown to induce the same or similar secondary structures in many small peptides and proteins, though membrane-bound enzymes are rarely active in micellar media (Sanders and Landis, 1995). Furthermore, the curvature of the micelle surface is quite different from more planar lipid bilayers.

Often, knowledge of the secondary structure of the peptide induced by micelles is generated by the incorporation of NMR-derived distance restraints into either a simulated annealing (SA) or a distance geometry procedure. SA is usually done in vacuo or by using a distance-dependent dielectric constant. From this information deductions are made as to the structure of the peptide-micelle complex and occasionally about the dynamics of the peptide. However, in most cases (for small peptides), the peptides are known not to possess the secondary structure observed in the micellar medium in the absence of micelles. The nature of the actual micellar environment (lipid core, interfacial region, and surrounding solvent) and the effects of the environment on the secondary structure and dynamics of the peptide cannot be easily reproduced without the use of explicit solvent models. Guba and Kessler (1994) have used a biphasic simulation cell consisting of water and carbon tetrachloride for molecular dynamics (MD) studies of peptides in membrane mimics to provide a better model of the hydrophilic/hydrophobic interface that more realistically includes the effect of an interfacial environment on the properties of the peptide. This model system gives an approximation about the orientational/positional properties of the peptide with respect to the membrane interface. The preceding paper also demonstrated the merits of this protocol. Yet, the biphasic cell leaves out the representation of the headgroup, with which interaction of the peptides may be significant. Furthermore, the interfacial region can be quite broad, possessing its own unique characteristics (Weiner and White, 1992) while the water/carbon tetrachloride interface was relatively sharp. In this work the results of MD simulations of two peptides, substance P (SP) and its tyrosine-8 analog (SP-Y8), in an explicit sodium dodecylsulfate (SDS) micelle are reported. The SDS system is one of the two most commonly

Received for publication 12 June 1998 and in final form 24 November 1998.

Address reprint requests to Dr. Tuck C. Wong, Department of Chemistry, University of Missouri, 123 Chemistry Building, Columbia, MO 65211. Tel.: 573-882-7725; Fax: 573-882-2754; E-mail: chem1060@showme.missouri.edu.

0006-3495/99/03/1213/15 $2.00

used micellar mimics for high resolution NMR studies. The results from these simulations can be compared to experiments for these peptides in the same micellar systems in a more direct fashion. At the time of this writing, there was no report of any MD simulation of a peptide interacting with an explicit micelle in the literature. A preliminary report (Woolf et al., 1998) on MD simulations of the transmembrane portions of glycophorin, both the monomer and the dimer, in dodecylphosphocholine (DPC) micelles has been presented.

To understand the physical and structural properties of membrane-bound peptides and proteins and their relationship to the biological activities, MD simulations with ever-improving force fields and longer time scales have been providing molecular level details of such systems. MD simulations on lipid bilayer spanning proteins with explicit representation of the lipid bilayer have recently appeared in the literature (Shen et al., 1997; Belohorcova et al., 1997; Woolf and Roux, 1996; Merz, Jr. and Roux, 1996). For peptides too short to span the membrane bilayer, the interactions with the membrane may be different. Damodaran and Merz (1995) presented MD simulations on the fusion-inhibiting peptide carbobenzoxy-D-Phe-L-Phe-Gly with a N-Me-DOPE bilayer that revealed a possible molecular mechanism for fusion inhibition. Damodaran et al. (1995) carried out MD simulations of the tripeptide Ala-Phe-Ala-O-tert-butyl with a dimyristoylphosphatidylcholine lipid bilayer. The peptide-lipid interactions from the MD simulation were in agreement with experiment (Brown and Huestis, 1993; Jacobs and White, 1989). Huang and Loew (1995) reported simulations on residues 13–41 of the amphipathic helical peptide corticotropin-releasing factor (CRF) in a DOPC bilayer. Zhou and Schulten (1996) investigated the complex of phospholipase A_2 on the surface of a lipid membrane which provided explanations on the enhanced activity of the enzyme once membrane-bound. Kothekar (1996) reported a MD simulation on the SP peptide in a lipid bilayer. The simulation was carried out with an initial configuration that had the peptide inserted into the lipid region perpendicular to the interface. The simulation time of 260 ps was most likely insufficient to reveal the equilibrated position/orientation of the peptide if it was initially placed in an unfavorable orientation and position (see the Equilibration section).

SP is an 11-residue neuropeptide with the sequence RP-KPQQFFGLM-NH_2. SP-Y8 has the single substitution of Tyr for Phe at the eighth residue (Fisher et al., 1976). The biological properties of SP and SP-Y8 have been described in the preceding paper. SP has also been well studied experimentally in solution, in lipid bilayers, and in micellar media (see preceding paper) and therefore serves as a good model to test our methods. In addition, the results obtained from peptides placed in the biphasic cell and in the explicit SDS micelle will be compared and contrasted, and the validity and utility of the biphasic cell as an approximation for micellar or bilayer systems are examined.

METHODS

MD simulation details

The CHARMM program (Brooks et al., 1983) version 24b2 was used for all minimizations and simulations of the explicit peptide-SDS micelle system. The CHARMM all22 force field was used for the peptide (MacKerell et al., 1998) and the lipids (Schlenkrich et al., 1996). The water model used was TIP3P (Jorgenson et al., 1983). All minimizations and MD simulations were performed in the *NVT* ensemble (see Discussion) with the application of periodic boundary conditions. Velocities were scaled if the temperature was not within 10 of 300 K checked every 50 steps. This procedure was never called for after 50 ps of equilibration. The integration time step was 1 fs with bonds to hydrogen atoms constrained to a fixed value by SHAKE (Ryckaert et al., 1977). The long-range forces were handled by using a force switch from 8 to 10 Å. This method of handling long-range forces leaves short-range forces unaltered and damps forces monotonically to zero in the interval from r_{on} to r_{off}. The minima and barriers introduced by force switching are considerably less pronounced than those caused by potential switching (Steinbach and Brooks, 1994). In addition, using this method for the nonbonded interactions does not require that we couple the solvents and the peptide to separate temperature baths to produce uniform temperature (Oda et al., 1996). The nonbonded list was updated every 20 steps.

Construction of initial MD conditions

The initial coordinates for the solvated SDS micelle, which contains 60 dodecylsulfate monomers, 60 sodium ions, and 4398 waters for a total of 15,774 atoms resulting in a cubic system of 54.1 $Å^3$, was kindly provided by Dr. A. MacKerell (MacKerell, 1995). Since our simulations were performed in the *NVT* ensemble, the initial estimates of the dimensions and density of the membrane media must be accurate (Jakobbsen et al., 1996) to reproduce experimental aspects of the membrane structure. The number of SDS monomers is in agreement with the experimental aggregation number of 62 (Croonen et al., 1983; Attwood and Florence, 1983). The density profiles for carbon and sulfur are in good agreement with the experimental paraffinic radius of 16.7 Å and the total radius of 22.3 Å from x-ray scattering (Itri and Amaral, 1991) and from NMR (Soderman et al., 1988). Recent simulation results from our laboratory for another peptide of similar size (adrenocorticotropin (1-10)) in a solvated SDS micelle done at constant pressure and temperature suggest that the size of the cubic system should be ~53.7 $Å^3$, which is slightly contracted from 54.1 $Å^3$. Therefore, the internal pressure of our system would be slightly negative but most likely still a reasonable value.

Results from simulations of SP and SP-Y8 in the biphasic cell clearly demonstrated that the SP peptides equilibrated to the interface and become oriented parallel to the interface even if the peptide backbone was originally inserted into the hydrophobic phase perpendicular to the interface (see preceding paper). In order to verify that the same resulting orientation will prevail for a peptide inserted into the *micellar* core, the following configuration was constructed. The SP-Y8 peptide was inserted into the micelle lipid core with Pro-4 located at the headgroup region in a secondary structure from SA (see preceding paper for details). Residues preceding Pro-4 in the sequence were mostly in contact with water. Residues following Pro-4 in the sequence were in contact with the lipids. Three lipids and 42 waters were deleted to create space for the peptide. Six Na^+ counterions closest to the peptide and three lipids were deleted to maintain electrical neutrality. The initial configuration of the peptide-micelle complex with the peptide inserted into the lipid's interior is shown in Fig. 1.

The MD of SP-Y8 inserted into the micelle core (carried out before the SP in SDS simulation) equilibrated to the surface of the micelle (see Results). Based on this result and results from SP in the biphasic cell, SP was placed on the surface of the micelle with a secondary structure from SA (see preceding paper for details) to reduce the equilibration time. Residues that were in contact with the carbon tetrachloride throughout the biphasic cell simulation were placed in contact with the lipids. The heter-

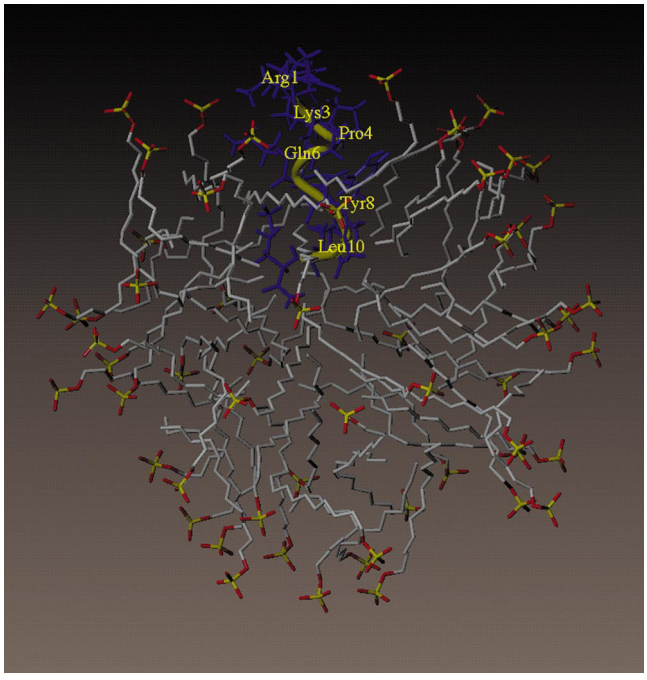

FIGURE 1 Starting configuration of SP-Y8 partitioned in SDS micelle [SP-Y8 (*blue*), hydrocarbon chains (*gray*), sulfur (*yellow*), and oxygen (*red*)]. The peptide is inserted into the micelle hydrophobic core from Pro-4 to Met-11. The hydrogen atoms on the lipids, TIP3P water, and sodium counterions have been deleted for clarity. A yellow ribbon traces the peptide backbone.

ogeneity of the micellar surface makes placing peptides at the micellar interface a challenge, because the choice of water/lipid molecules to delete can greatly affect the shape of the micelle (see Roux and Woolf, 1996 for construction of protein/lipid bilayer configurations). After placing SP on the surface of the SDS micelle, overlapping waters and the three closest Na^+ counterions were deleted due to the +3 charge on SP. The system was heated to 300 K by scaling of the velocities over 3 ps, NOE restraints of 10 kcal/(mol · Å) on the peptide. The simulation was continued for 40 ps at which time three lipids, which were somewhat separated from the micelle, were deleted along with the closest three Na^+ counterions. The final system contained about the same number of atoms from the original SDS micelle system and the SP-Y8-micelle system. Deletion of three lipids was required to maintain a similar density, yet deletion of even one lipid would have an effect on the characteristics of the micelle unless volume adjustments are made by simulating in the *NPT* ensemble. The fact that three lipids became separated from the micelle to varying degrees made the choice of which lipids to delete much easier and resulted in a more spherical micelle. Penetration of water into the micellar core was not observed.

Both systems were minimized by 2000 steps of steepest descent using a 10-Å nonbonded cutoff. The structure of the peptide was restrained by force constants of 10 kcal/(mol · Å) corresponding to strong (2.0–2.7), medium (2.0–3.0), and weak (2.0–3.3) NOE correlations in the two-dimensional (2D) NMR (see preceding paper). These restraints were kept throughout the equilibration and beyond. The MD was started by heating to 300 K in increments of 10 by scaling of the velocities over 3 ps.

MD simulations with no restraints on peptide

The unrestrained simulation of the SP/micelle system was started from coordinates taken at 95 ps of the restrained trajectory. The system was heated to 300 K as mentioned above with NOE restraints on the peptide. The restraints were removed and the trajectory was continued for 1.04 ns. Removal of the restraints may cause some relaxation of the peptide and therefore the first 40 ps of the unrestrained trajectory is neglected in the analysis. Snapshots of the trajectory were taken every 250 fs. The SP-Y8 simulation was carried out for 1 ns without restraints starting from the final coordinates of the restrained dynamics. The first 30 ps of the trajectory were also neglected due to relaxation of the peptide from removing the restraints. Snapshots of the trajectory were taken every 250 fs.

RESULTS

Equilibration of the peptide-micelle complex

The SP/micelle system originally oriented parallel to the micellar surface was equilibrated for 120 ps. Analysis of the restrained dynamics was made over the subsequent 280 ps with snapshots of the trajectory taken every 500 fs. The total simulation time was 400 ps. Fig. 2 *A* shows the typical configuration of the SP peptide-micelle complex over the restrained simulation. The peptide remained almost parallel to the micellar surface. The hydrophobic side chains of Lys-3, Pro-4, Phe-7, Phe-8, Leu-10, and Met-11 are clearly in contact with the interface or the hydrophobic core regions, whereas those of Arg-1, Pro-2, Gln-5, Gln-6, and Gly-9 are in contact with water.

The SP-Y8 simulation with the initial insertion configuration showed virtually no change for ~200 ps, at which time the peptide backbone began to orient at an angle with respect to the local interface. By 400 ps, the SP-Y8 peptide backbone had moved out of the micellar core and had oriented parallel to the micelle surface except for the last residue, Met-11, which was still mostly in the micellar core. The carbonyl oxygen of Met-11 had formed an intramolecular hydrogen bond with the Leu-10 NH. This hydrogen bond was broken at 450 ps, when the backbone of Met-11 was solvated by water and was positioned at the interface instead of the micellar core. Fig. 2 *B* shows the typical configuration of the SP-Y8 peptide-micelle complex during the last 210 ps of the restrained dynamics. With the exception of the side chains of Pro-4 and Tyr-8, the positioning of the side chains in the various regions of the micelle is quite similar to that of SP (this point will be discussed in more detail later). The simulation was continued for another 300 ps, for a total of 750 ps. The last 210 ps was used for analysis of the restrained dynamics. Snapshots were taken every 500 fs for analysis.

The equilibration of the SP-Y8 peptide to the surface of the micelle from an inserted configuration required over 400 ps, and we observed virtually no change in the orientation of the peptide with respect to the micellar surface until after 200 ps. The present result is consistent with the suggestion that small peptides unable to traverse a lipid core region are usually less likely to be inserted into the bilayer because of the necessity of exposing some polar peptide bond to the hydrophobic interior (Ben-Tal et al., 1996; Wimley and White, 1996). Thus they should not be simulated in an insertion mode unless there is specific experimental information to suggest that the peptide is inserted into the lipid region or if one is willing to equilibrate for long periods,

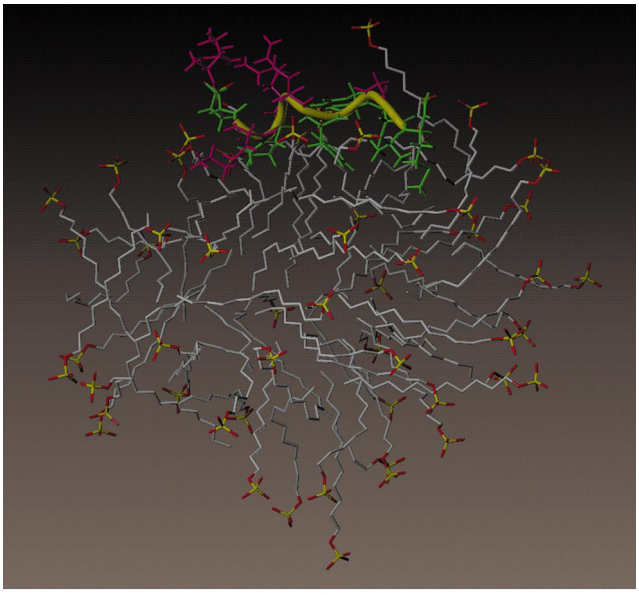

A

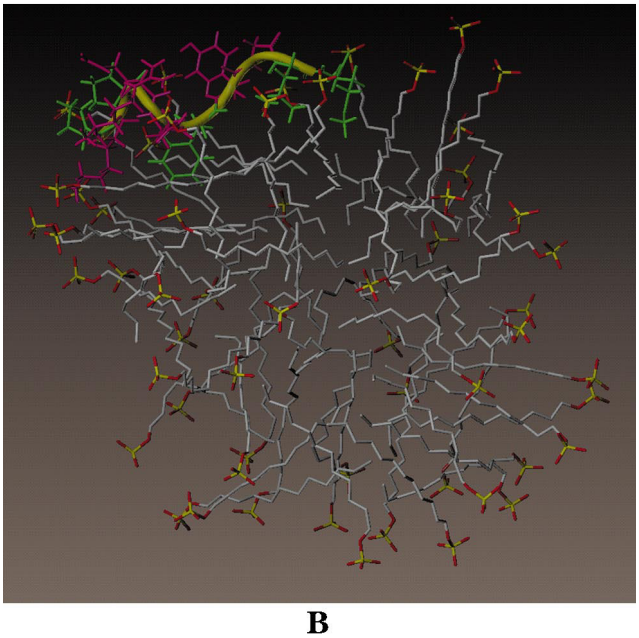

B

FIGURE 2 SP (*A*) and SP-Y8 (*B*) on the surface of the SDS micelle in an equilibrium configuration after 360 and 600 ps of simulation, respectively [hydrophobic residues (*green*), polar residues (*red*), sulfur/oxygen of the lipid headgroup (*yellow/red*), lipid methylene chains (*gray*)]. The hydrogen atom on the lipids, TIP3P water, sodium counterions, and a few lipids have been deleted for clarity. A yellow ribbon traces the peptide backbone.

i.e., 500 ps or more. The resulting orientation of SP-Y8 parallel to the micelle surface is in agreement with experimental results for SP (Young et al., 1994; Seelig and Macdonald, 1989; Duplaa et al., 1992). However, Schwyzer (1992) suggested that SP was oriented perpendicular to the membrane surface with ~7–8 residues inserted into the hydrophobic core. The degree of hydration of the bilayers may have been a determining factor in Schwyzer's studies (Frey and Tamm, 1991). However, Schwyzer et al. based their conclusions on results for SP in lipid bilayers of low hydration (by ATR-IR), and SP in vesicles that have a high degree of hydration (by photoaffinity labeling). There appeared to be no distinction made between the results from these two systems (Schwyzer, 1992).

The equilibration was followed by additional RMD and free MD simulations, as described in the Methods section. The analyses of several important properties of the peptide-micelle system from the RMD or the free MD trajectories are presented as follows.

Conformation of SP peptides

The restrained simulation of SP was analyzed from 118 to 398 ps. This structure consisted of two type I β-turns (Wilmot and Thornton, 1990) from Pro-2 to Gln-5, from Lys-3 to Gln-6, and an extended turn that does not conform to any specific type of β-turn from Gln-5 to Phe-8. The secondary structure of the midregion of the peptide, from Pro-4 through Phe-8, is in agreement with other studies of SP (Williams and Weaver, 1990; Woolley and Deber, 1987; Keire and Fletcher, 1996). Our results extend the secondary structure to Pro-2. The N-terminal residues, Pro-2 through Pro-4, have not previously been assigned a secondary structure, perhaps due to the absence of the amide proton on the proline residues which limits the amount of data generated from 2D NOESY experiments. Intramolecular hydrogen bonds with an acceptor-donor-hydrogen distance of <2.8 Å and an acceptor-hydrogen-donor angle $>120°$ (Ravishanker et al., 1994) were present between Pro-2 oxygen and Gln-5/Gln-6 amide hydrogen, Lys-3 oxygen and Gln-6/Phe-7 amide hydrogen, and between Phe-7 oxygen and Leu-10 amide hydrogen. The donor for Pro-2 and Lys-3 oxygen fluctuated between the given acceptors. The 1-ns simulation of SP without restraints shows two conformations due to a conformational transition at ~400 ps. The peptide during the first part of the simulation before the conformational transition adopts a distorted (due to Pro-4) α-helix from Lys-3 to Phe-7. This secondary structure is not far removed from the secondary structure obtained from RMD. The difference in the ϕ-ψ values between consecutive type I β-turns and an α-helix is minimal when the appreciable flexibility of small peptides is taken into consideration. After the conformational transitions for ϕ of Gly-9 and ψ of Gln-6 and Phe-8, the only identifiable secondary structure conserved is the type I β-turn from Pro-2 to Gln-5. This secondary structure does not resemble any reported in the literature. However, such extensive MD simulations have not been carried out previously for SP and it is not clear how long such a secondary structural element persists and therefore how much it will contribute to the time-averaged conformation observed in experiments. Analysis of proton-proton distances corresponding to the medium range NOEs reveals that after the conformational transition in the free MD, the Gln-5 Hα–Phe-8 NH and Gln-6 NH–Phe-8 NH

distances average 7.2 Å and 6.3 Å, respectively, apparent violations of the NOE. The RMD averages for the distances between these two proton pairs were 4.2 Å and 4.7 Å, respectively. Other RMD-MD differences were due to the increased distances between the side chains of Gln-5 and Phe-8 and of Phe-7 and Leu-10 in the free MD. However, these side chain pairs remained in similar micellar environments in the free MD and thus the amphipathic structure remained. The ϕ-ψ values and the root-mean-squared (rms) fluctuations are given for SP during the restrained MD and during the last 450 ps of the free MD (after the conformational transition) in Table 1. The carbonyl oxygen of Lys-3 was mostly hydrogen-bonded either to Gln-5 or Gln-6 amide hydrogen throughout the entire simulation, while other intramolecular hydrogen bonds fluctuated over the unrestrained simulation, making specific analysis of hydrogen-bonding partners less meaningful.

The restrained simulation of SP-Y8 was analyzed from 530 to 750 ps. The secondary structure over this period shows that residues Lys-3 through Phe-7 form an α-helix (see Table 2) with some distortion caused by Pro-4. These results are in partial agreement with a study by Gao and Wong (submitted for publication) who suggested, based on 2D NMR, that SP-Y8 in SDS micelles is helical from Pro-4 to Gly-9. However, the MD simulation results (both restrained using similar NOE restraints and unrestrained) show the helix terminating at Tyr-8, which places it in better contact with the aqueous environment than would be the case if Tyr-8 were part of the helix. The only significant RMD-MD differences in proton-proton NOE distances were between the side chain protons of Gln-5 and Tyr-8 and between Phe-7 and Leu-10, even though the side chain pairs remained in the aqueous and micellar core regions, respectively; thus the amphipathic structure remained. Intramolecular hydrogen bonds were present between Pro-2 oxygen and Gln-5/Gln-6 amide hydrogen, Lys-3 oxygen and Phe-7 amide hydrogen, and between Gln-5 oxygen and Tyr-8 amide hydrogen. The donor for Pro-2 oxygen fluctuated between the given acceptors. The 1-ns free MD simulation of SP-Y8 showed that the peptide remains in this same secondary structure. However, the fluctuations are quite large (see section on dynamics) with the ψ angle of Phe-7 and the ϕ angle of Tyr-8 moving toward more negative values. This secondary structure is slightly different than the one obtained with simulations in the biphasic cell, which showed only Gln-6 and Phe-7 having α-helical values while the rest of the peptide existed in extended turn structures. The difference is most likely due to electrostatic interactions that place the charged segment of SP-Y8 in closer contact with the interface and resulting in a more defined secondary structure. No conformational transition was observed over the Lys-3 through Tyr-8 section in the unrestrained simulation, but the Gly-9/Leu-10 backbone section is more flexible than the other residues based on ϕ-ψ rms fluctuations.

One side chain-side chain interaction observed in the simulations of SP and SP-Y8 in the SDS micelle was that between Gln-5 O_ϵ and protons bonded to the nitrogen atoms of the Arg-1 side chain. Though the proton donors fluctuated, in many snapshots this interaction was shown to be in a bifurcated configuration. This interaction could constrain the motion of the Gln-5 side chain and reduce the T_2 of the side chain protons. This may be the reason for the particularly weak TOCSY signals for this residue for both peptides in the SDS micelles (Gao and Wong, submitted for publication).

TABLE 1 Average ϕ-ψ values for SP partitioned in an SDS micelle during the RMD (118–398 ps) and free MD (the last 450 ps) simulations

	RMD		MD	
SP	ϕ	ψ	ϕ	ψ
Arg-1	NA	149.2 (10.9)	NA	158.2 (11.6)
Pro-2	−79.9 (7.1)	178.3 (5.8)	−71.2 (8.6)	163.9 (13.1)
Lys-3	−73.5 (8.9)	−32.4 (7.2)	−59.0 (11.5)	−34.6 (9.8)
Pro-4	−70.9 (7.2)	−5.3 (7.4)	−67.9 (7.5)	−5.6 (10.1)
Gln-5	−105.9 (8.4)	−1.3 (9.5)	−108.4 (13.0)	**−61.2** (9.5)
Gln-6	−73.6 (11.4)	−47.9 (7.4)	−79.7 (9.7)	**72.4** (12.7)
Phe-7	−92.2 (9.3)	29.6 (6.6)	−75.2 (12.6)	**−49.7** (14.3)
Phe-8	−69.3 (8.3)	3.2 (17.7)	−78.7 (11.4)	**155.5** (19.9)
Gly-9	−154.5 (19.1)	60.6 (8.9)	**96.8** (23.2)	31.7 (25.6)
Leu-10	−61.6 (8.4)	148.1 (9.4)	**−97.6** (24.1)	177.3 (14.3)
Met-11	90.6 (16.3)	NA	90.7 (16.6)	NA

Values in bold show changes from the RMD of over 30°; rms fluctuations are in parentheses.

TABLE 2 Average ϕ-ψ values for SP-Y8 partitioned in an SDS micelle during the RMD (530–750 ps) and free MD (the last 1000 ps) simulations

	RMD		MD	
SP-Y8	ϕ	ψ	ϕ	ψ
Arg-1	NA	169.4 (7.3)	NA	**138.1** (17.9)
Pro-2	−63.0 (6.4)	168.1 (6.4)	−75.2 (9.1)	172.8 (8.2)
Lys-3	−43.5 (9.2)	−49.4 (7.3)	−50.3 (12.9)	−49.0 (11.3)
Pro-4	−72.6 (7.0)	−35.4 (7.2)	−70.6 (7.8)	−8.9 (11.0)
Gln-5	−80.6 (8.3)	−23.3 (7.1)	−95.0 (12.6)	−49.7 (9.4)
Gln-6	−38.0 (9.6)	−56.3 (8.2)	−38.2 (12.1)	−55.3 (11.2)
Phe-7	−75.2 (12.1)	−68.6 (7.1)	−78.4 (11.2)	−70.2 (18.1)
Tyr-8	−25.1 (10.0)	112.9 (9.5)	**−75.5** (18.5)	**151.0** (18.1)
Gly-9	−84.1 (11.0)	39.2 (8.8)	**102.3** (28.7)	**8.1** (34.2)
Leu-10	−73.8 (9.1)	168.0 (7.5)	−87.5 (23.7)	158.3 (12.4)
Met-11	74.4 (9.9)	NA	78.8 (12.7)	NA

Values in bold show changes from the RMD of over 30°; rms fluctuations are in parentheses.

Peptide-solvent properties

The analysis of the solvation of the peptide backbone was facilitated by calculating the radial distribution functions (RDF), g(r), between the SP peptide backbone carbonyl oxygen with the oxygen atoms of water (Fig. 3), the associated hydration numbers, and the position of the first hydration peak. The results are presented in Table 3. Since the polarity of the peptide backbone stems largely from the carbonyl group and the energetic cost of inserting the pep-

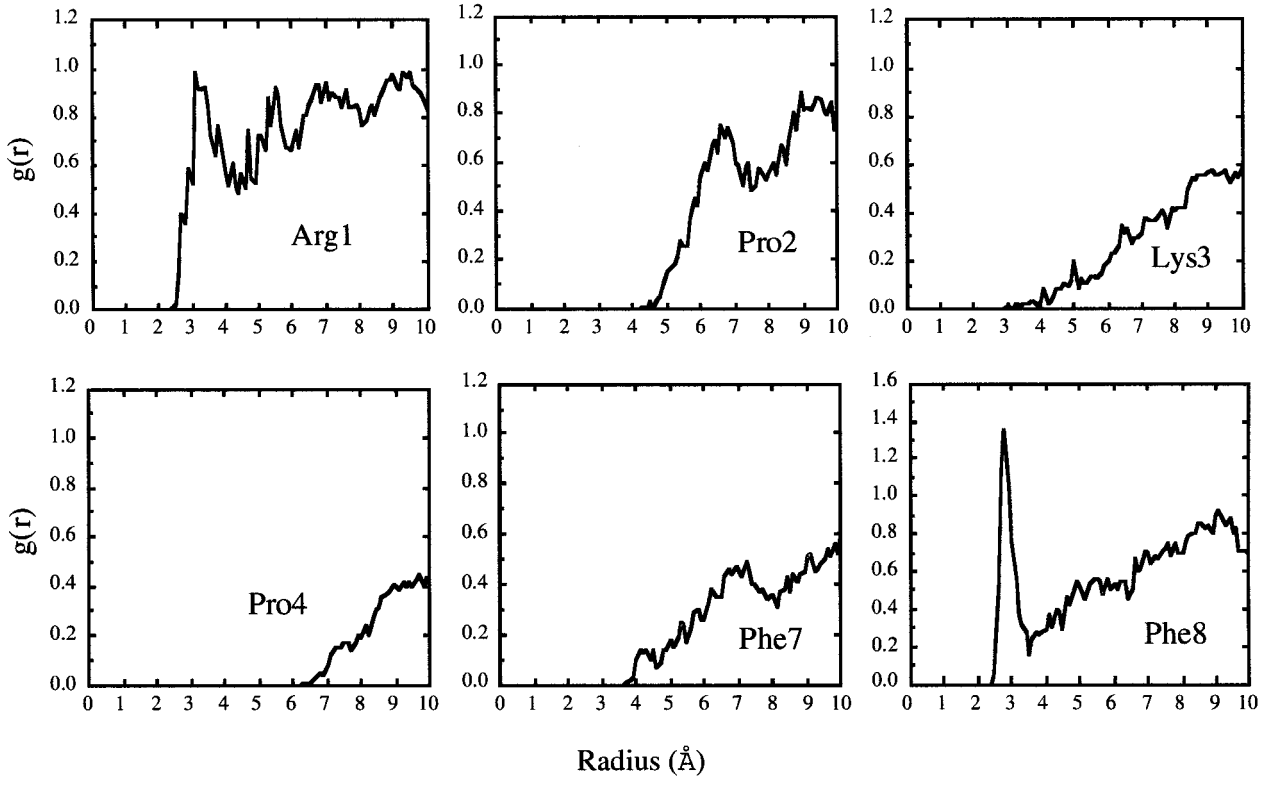

FIGURE 3 RDFs of SP carbonyl oxygen with the oxygen atoms of water over restrained trajectory (120–400 ps). Residues not shown have an RDF similar to Phe-8, i.e., having a strong solvation peak, indicating the solvation of the carbonyl group by water.

tide bond into the lipid region has been estimated to be 5–6 kcal/mol (Roseman, 1988), these RDFs can be quite revealing as to the nature of the peptide interactions with the micellar surface or hydrophobic core. The peptide solvent RDFs were examined for the SP-SDS micelle system over the restrained dynamics, the initial 356 ps, the final 400 ps, and over the entire unrestrained simulation of 1 ns. This procedure was used because of the conformational transition that took place at ~400 ps. During the restrained simulation, the backbone of SP (except for Pro-4) was either solvated or involved in intramolecular hydrogen bonds, as was the case for simulations carried out in the biphasic cell. The only difference in the RDFs was that all the g(r) values were lower in the SDS simulation than in the biphasic system (compare Fig. 3 with Fig. 6 of preceding paper). This reduction in g(r) values was interpreted as being due to the peptide residing in the interfacial region distinct from either the micelle core or the bulk solvent surrounding the micelle. This interfacial region is more heterogeneous than the relatively sharp interface found in the water/carbon tetrachloride interface. During the first 350 ps of the unrestrained simulation, there are minor decreases in the value of g(r) for the first solvent shell of Gln-6 and Phe-8 (results not shown) from the restrained simulation. The change in Pro-4 and Phe-7 during the first 350 ps showed both residues developing a primary solvent shell (Fig. 4). This increase in the value of g(r) of the primary solvent shell continued throughout the simulation, as seen in the RDF over the last 400 ps of the trajectory (Fig. 4). It is not certain whether these results indicate the peptide-micelle configuration is still equilibrating or these are slow fluctuations. Overall, the analysis showed that the backbone is either involved in intramolecular hydrogen bonds or is solvated by water (Fig. 3 and Table 3). This can be considered as an important factor favoring the orientation of the peptide parallel to the interface region. The side chain atoms that are immersed in the hydrophobic part of the micelle are Pro-4, Phe-7, Phe-8, Leu-10, and Met-11 (Fig. 5). During the

TABLE 3 Hydration numbers for the peptide carbonyl oxygen atoms with oxygen atoms of water from RDFs shown in Fig. 3

Residue	First Peak Position (Å)	Integrated to (Å)	Hydration No.
Arg-1	3.1	4.4	1.19
Pro-2	—	**5.0**	**0.03**
Lys-3	—	**5.0**	**0.09**
Pro-4	—	5.0	0.00
Gln-5	2.8	3.4	0.42
Gln-6	2.8	3.4	0.76
Phe-7	—	**5.0**	**0.13**
Phe-8	2.8	3.4	0.63
Gly-9	2.8	3.4	0.82
Leu-10	2.8	3.4	0.50
Met-11	2.8	3.4	0.93

Residues in bold participate predominately in intramolecular hydrogen bonds.

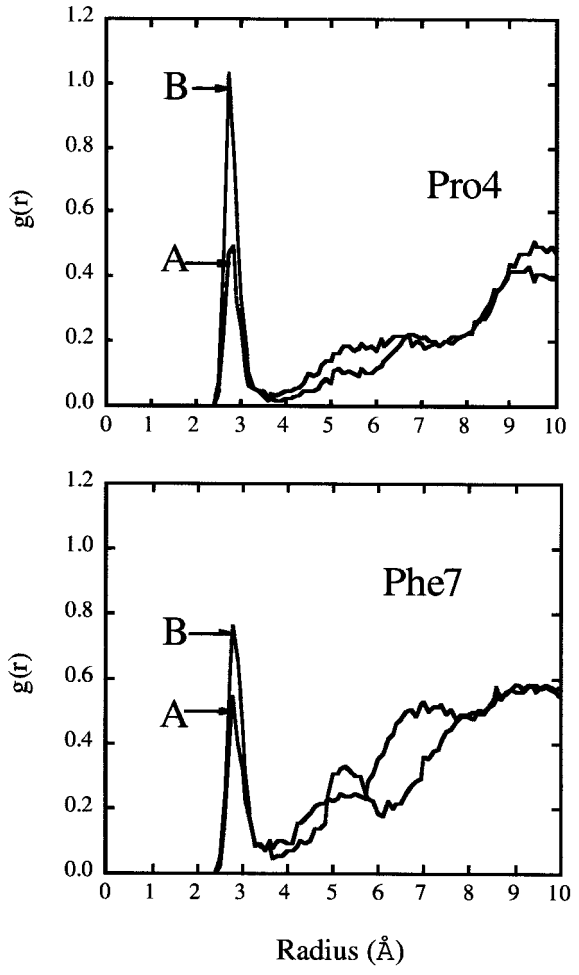

FIGURE 4 The RDFs between the carbonyl oxygen atom of Pro-4 (*top*) and Phe-7 (*bottom*) and the oxygen atoms of water over the course of the unrestrained dynamics. *A*, first 350 ps; *B*, last 400 ps. The changes in the RDF showed the development of the solvation shell around the carbonyl oxygen atoms.

simulation, the aromatic side chains moved away from being inserted into the micelle core to being directly at the interface. Neither the Phe-7 or Phe-8 side chains develops a primary solvent shell consistent with the hydrophobicity of these side chains (Wimley and White, 1996). The preference of aromatic residues for the membrane interfacial region has been shown experimentally and also in another simulation (Wimley and White, 1996; Woolf, 1998) though the exact physical interactions for this interfacial preference have not yet been well characterized. The methylenes of Lys-3 were shown to be in a hydrophobic environment in a configuration reminiscent of the "snorkel effect," where the methylenes of Lys-3 make contact with the methylenes of the lipids and the charged terminal amino group of Lys-3 curling up so as to be solvated by water (Segrest et al., 1990).

The RDFs, the associated hydration numbers, and the position of the first hydration peak between the backbone carbonyl oxygen and the oxygen atoms of water for SP-Y8 in SDS were examined over the restrained dynamics from 531 to 750 ps (Fig. 6 and Table 4). When comparing these RDFs with the respective RDFs for SP-Y8 in the biphasic simulation cell, it was observed that the well-defined primary solvent shell for the first three residues was absent due to a major reduction in the g(r) values (compare Fig. 6 with Fig. 9 of preceding paper). This is certainly due to this interaction between the charged segment and the charged micellar headgroup, which brings this section into the interfacial area. The detailed description of the interaction of these residues with the SDS headgroups will be presented in Peptide-headgroup interactions. Representation of the charged headgroups is neglected in the biphasic cell model, and thus the effects of the interactions of the peptides with the headgroups will not be revealed in the MD results.

Since SP-Y8 did not show any conformational transitions over the 1-ns trajectory, the RDFs presented were calculated over the last 1 ns of the trajectory. As is the case in the SP simulation, the carbonyl of Pro-4 developed a primary solvent shell. The fact that this occurs also in the simulations of SP seems to imply that the carbonyl of Pro-4 prefers to be solvated. Since Pro-4 does not undergo any conformational transition to attain this solvent shell, and the peptide is not undergoing any diffusion away from the micelle, water must be penetrating this particular area. As was the case for simulations of these peptides in the biphasic cell, one major difference between the two peptides is the interaction of the aromatic side chains with the hydrophobic region. The side chain of Phe-7 in both peptides is clearly in the hydrophobic region, while that of the Tyr-8 of SP-Y8 is solvated by water and Phe-8 of SP is not solvated, or at least to a much smaller extent (Fig. 7). Furthermore, aromatic-aromatic interactions are observed for the SP simulation due to the near parallel arrangement of the two aromatic rings. This interaction results in increased shielding of Phe-7 from water, though Phe-8 is no longer as shielded due to the movement of Phe-8 toward the interface. Such aromatic-aromatic stacking interaction was not found in SP-Y8 where the two aromatic rings are pointed into different orientation of the (approximate) helix. The Leu-10 and Met-11 side chains are also in a hydrophobic or interfacial region of the micelle (Fig. 7).

Peptide-headgroup interactions

By analysis of the distribution of sulfur atoms of the micelle headgroups around each nitrogen of the charged peptide amino groups, we can make distinctions between the nonspecific (solvent-separated) and specific (hydrogen-bonded) electrostatic interactions. Both SP and SP-Y8 have a +3 charge due to Arg-1, Lys-3, and the N-terminus. The analysis of the SP-Y8 trajectory revealed that all these charged amino groups interacted with the micelle headgroups. This interaction can be seen in Fig. 8, which shows the RDFs between the sulfur atoms of SDS with the charged amino nitrogen atoms. The charged nitrogen of Lys-3 is shown to have four charged headgroups within 5 Å. Since the side

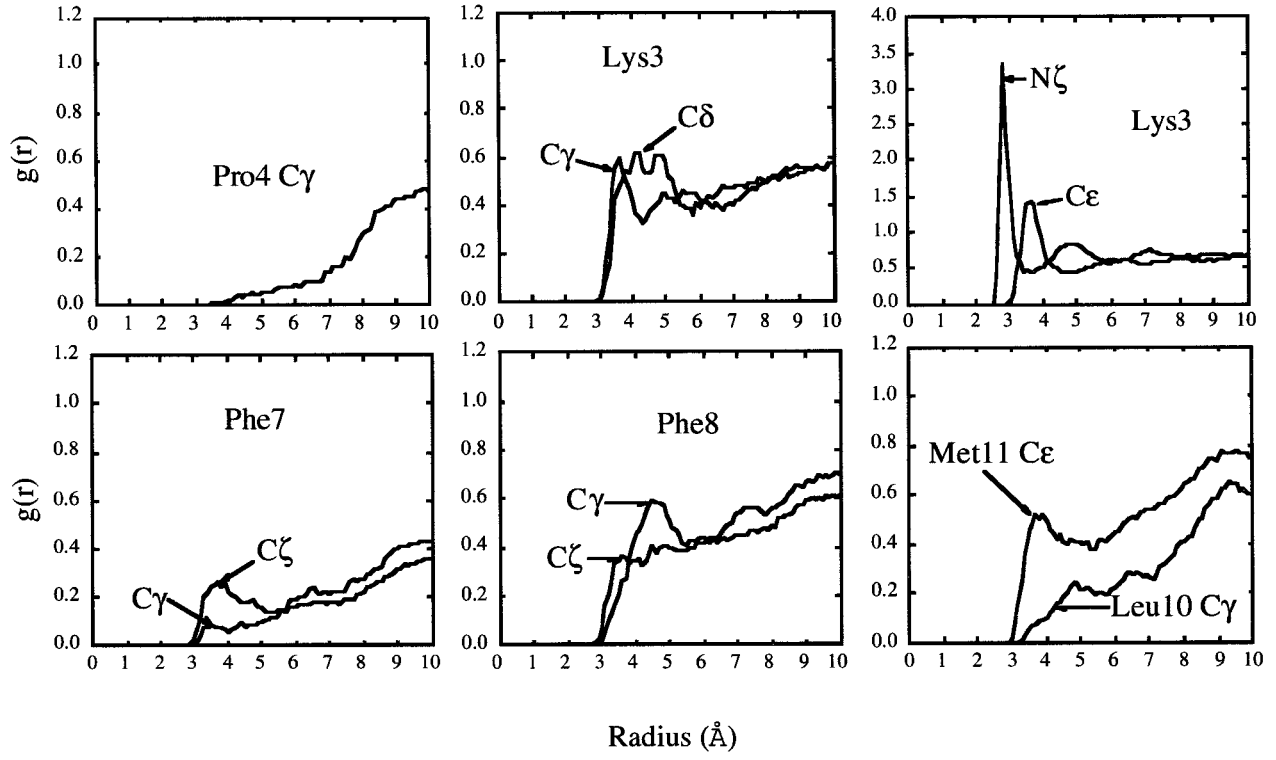

FIGURE 5 RDFs of selected side chain atoms with the oxygen atoms of water from the trajectory over the last nanosecond for SP in the SDS micelle.

chain of Lys-3 is immobilized due to the "snorkel effect" (see above), the Lys-3 charged amino group was prevented from interacting as much with the solvent. To compensate for the reduced solvent interaction, more sulfate groups interact with the Lys-3 amino group than the N-terminal amino group, which has more access to solvent. Specific hydrogen bonding between the N_ζ-H atoms and the oxygen atoms on the sulfate headgroup was observed. The hydrogen bonds fluctuate between different N_ζ-H atoms and the oxygen atoms on different sulfate headgroups of the SDS molecules. Significant hydrogen bonding with the sulfate oxygen atoms was also observed for the Gln-6 N_ϵH, the Tyr-8 phenolic hydrogen, the Met-11 NH, and one of the amidated C-terminal hydrogen atoms. The preference of tyrosine for an interfacial region may be due to this hydrogen bonding of the Tyr-8 phenolic hydrogen to the sulfate headgroup or other hydrogen bond acceptors (Wimley and White, 1996; Woolf, 1998).

SP does not show the same overall interaction with the lipid headgroups. The interaction between Lys-3 and the headgroup is the same as in SP-Y8. In addition, the Lys-3 NH, Gln-5 N_ϵ protons, Met-11 NH, and the C-terminal amide all show some hydrogen bonding with the micelle headgroups. The Lys-3 NH chemical shift changes in going from water to SDS micelles is 0.4 ppm, but only ~0.02 ppm in DPC micelles for both SP (Keire and Fletcher, 1996) and SP-Y8 (Gao and Wong, submitted for publication), suggesting a specific interaction with the sulfate headgroup in SDS. A large chemical shift difference is also seen for the Met-11 NH in going from aqueous solution to SDS or DPC micelles for both SP (Keire and Fletcher, 1998) and SP-Y8 (Gao and Wong, submitted for publication). Since the C-terminal section appears to lack any secondary structure, this chemical shift difference must be due to hydrogen bonding with the headgroups. Though DPC is overall uncharged, electrostatic interaction between the peptides with the headgroups cannot be completely ruled out. No other amide hydrogen atoms on the SP and SP-Y8 peptide backbone, with the exception of the amidated C-terminal, was observed to hydrogen-bond with the sulfate oxygen atoms throughout the entire 1-ns simulations, and their chemical shift differences between aqueous solution and SDS micelles may thus be attributed to secondary structure formation (see Conformation section). In Fig. 9, the RDF between the nitrogen atom in the backbone of Lys-3 and Met-11 and the sulfur atom on the SDS headgroup is shown. The peak in the RDF at 4.1 Å indicates the specific interaction, most probably hydrogen bonding between the NH protons and the sulfur oxygen atoms. No other amide nitrogen atoms on the rest of the residues exhibit such specific interaction in the RDF.

Dynamics of the peptide

Examination of the times series for the ϕ-ψ dihedral angles and their rms fluctuations for both SP and SP-Y8 from their respective 1-ns unrestrained trajectories was carried out to determine the flexibility of the various segments of the

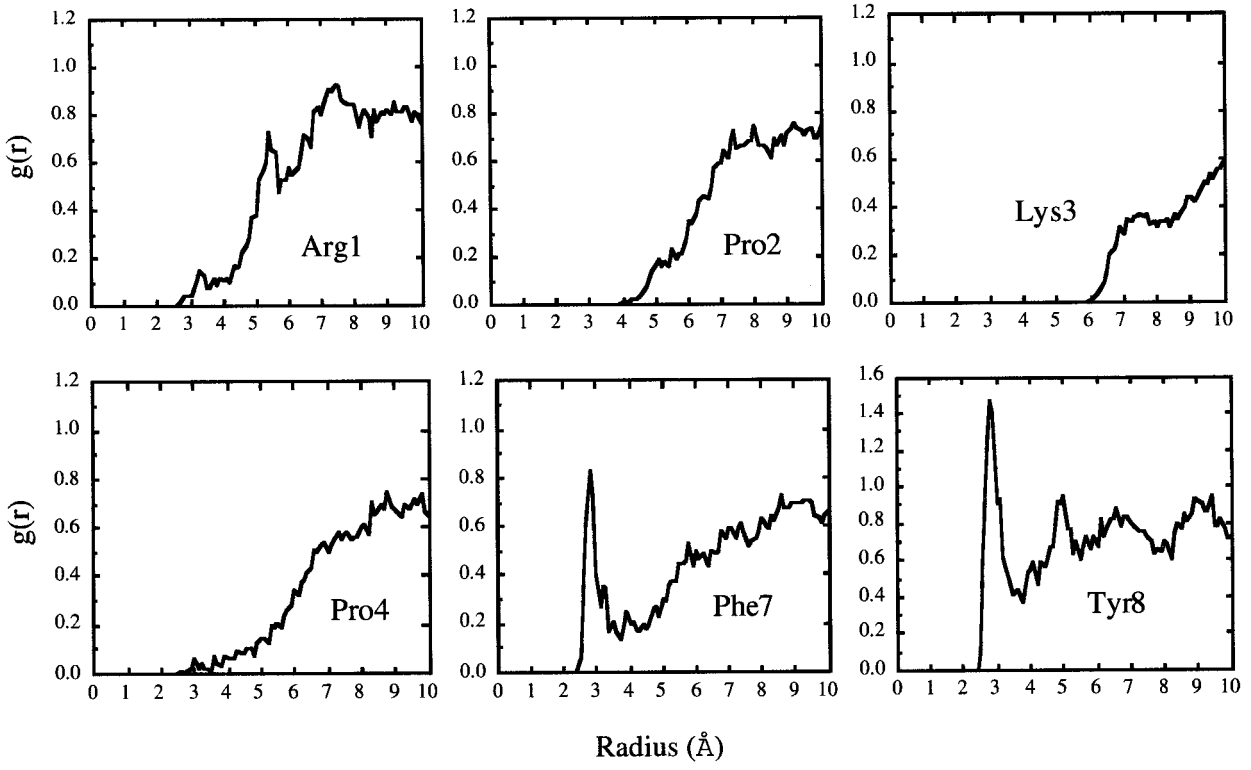

FIGURE 6 RDFs between the carbonyl oxygen atom with the oxygen atoms of water for SP-Y8 over the restrained trajectory (531–750 ps). Residues not shown have a RDF similar to Tyr-8, i.e., having a strong solvation peak, indicating the solvation of the carbonyl group by water.

peptides. SP undergoes a conformational transition at ~400 ps; one may infer from that the Gln-6 through Gly-9 section involved in the transition is more flexible if the peptide undergoes further conformation transitions back to the original conformation during the course of the simulation. However, since only one conformational transition is observed over the nanosecond trajectory, insufficient sampling does not permit such a conclusion. Fast fluctuations about the ϕ-ψ dihedral angles were well sampled over this period both before and after the conformational transition. Before the conformational transition, all the residues had roughly similar fluctuations of the dihedral angles. After the transition, the ψ of Tyr-8 and the ϕ of Gly-9 had larger rms fluctuations of 33.7° and 50.4°, respectively, while the other residues had an average rms fluctuation about the ϕ-ψ dihedral angles of 12.5° with a range of 9.5° to 20.9° (see Table 1). Glycine is known to be a residue that usually exhibits more flexibility than other residues in proteins and peptides and is often considered a helix breaker.

TABLE 4 Hydration numbers for the SP-Y8 peptide carbonyl oxygen atoms with oxygen atoms of water

Residue	First Peak Position (Å)	Integrated to (Å)	Hydration No.
Arg-1	3.3	4.4	0.17
Pro-2	—	**5.0**	**0.06**
Lys-3	—	**5.0**	**0.00**
Pro-4	—	5.0	0.14
Gln-5	**2.8**	**3.4**	**0.49**
Gln-6	2.8	3.4	0.59
Phe-7	2.8	3.4	0.40
Tyr-8	2.8	3.4	0.81
Gly-9	2.8	3.4	0.81
Leu-10	2.8	3.4	0.41
Met-11	2.8	3.4	0.74

Residues in bold are predominately in intramolecular hydrogen bonds.

In SP-Y8, the Gly-9/Leu-10 region is also more flexible than the rest of the peptide. The ϕ angles of Gly-9 and Leu-10 have the two largest rms fluctuations with values of 28.7° and 23.7°, respectively, while the average rms fluctuation in ϕ of the other residues is 12.1° with a range from 7.8° to 18.5°. The rms fluctuation in ψ of Gly-9 of 34.2° is almost twice as large as that of any other residue (see Table 2). Since the first three residues of SP have been proposed to be more flexible than the rest of the peptide (Convert et al., 1991), the ϕ-ψ dihedral angles of Gly-9/Leu-10 and of the first three residues were examined and their time series are shown in Fig. 10. While Arg-1 is slightly more flexible than Pro-2 and Lys-3, the Gly-9/Leu-10 region is clearly the most flexible. Interestingly, this flexibility is not extended to the Met-11 ϕ dihedral angle, perhaps because the Met-11 side chain is in contact with the lipids (see Fig. 7) with the NH and the amidated C-terminal hydrogen bonded with the oxygen atoms of the sulfate headgroup, as discussed earlier in the Peptide-headgroup interaction section.

Convert et al. (1991) proposed that the flexibility of the three N-terminal residues is a requirement for SP related

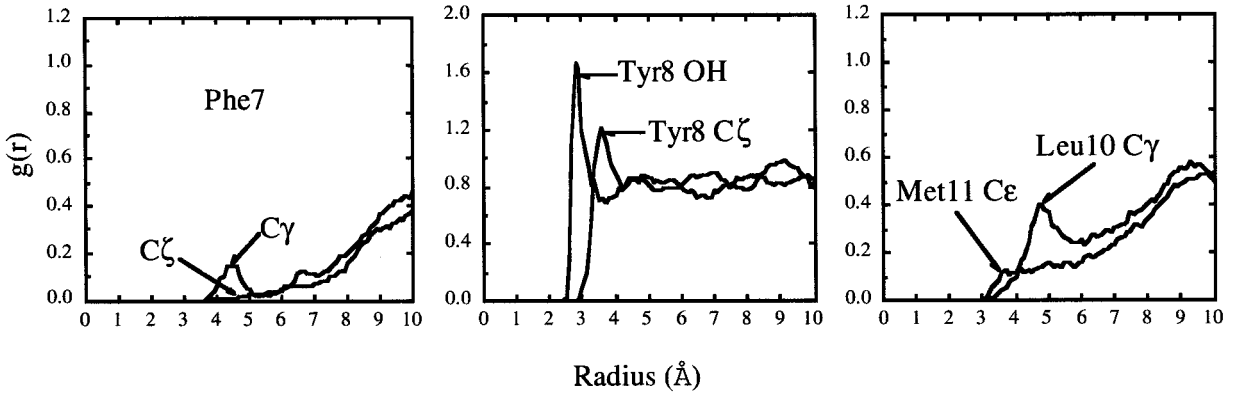

FIGURE 7 RDFs of selected side chain atoms with the oxygen atoms of water from the trajectory over the last nanosecond for SP-Y8 in the SDS micelle.

peptides to be biologically active. If indeed the first three residues must remain flexible for receptor activation, then the interaction between the peptide and an *anionic* lipid surface (the "natural membrane" contains ~25% of anionic lipids) should greatly reduce the flexibility of the first three residues, Arg-1 through Lys-3, and would have violated this requirement. Interacting with the membrane lipids as the first step in binding to the receptor is a major part of Schwyzer's (1992) membrane-mediated mechanism of receptor selection. The absence of intramolecular NOE correlations from 2D NMR for a certain segment of peptides has often been interpreted as meaning that particular segment of the peptide/protein is flexible. This inference may be reasonable for peptides in solution, but is quite suspect for peptides in micellar or similar environments. The interaction of segments of the peptide with the micelle (headgroup or hydrophobic regions) is not reflected in intramolecular NOE correlations, as demonstrated in this study. The presence of two prolines (Pro-2 and Pro-4) in SP peptides, and thus the lack of amide protons, near the N-terminus further reduces the chance of observing intramolecular NOE and deriving a secondary structure. Thus, the conclusion that the first three residues of SP in SDS micelles are flexible seems unwarranted from the experimental data and may only be resolved by examining the NMR relaxation times of these segments. Our simulation results are consistent with experimental NMR relaxation results for alamethicin oriented on the surface of SDS micelles (Spyracopoulos et al., 1996), which showed that the micelle tends to dampen out the flexibility of the peptide on the surface. Alamethicin was shown not to be as constrained as the core regions of

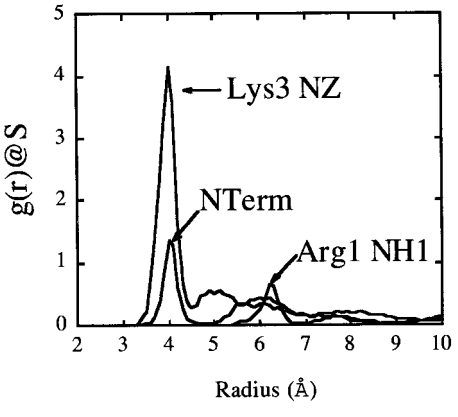

FIGURE 8 RDFs of charged amino nitrogen atoms of SP-Y8 with the sulfur atoms of SDS. The close contact between the other charged N atom of Arg-1 with the sulfate oxygen atoms is very similar to the contact between the N-terminal nitrogen atoms with the sulfate oxygen. Due to this overlap, the latter RDF is not shown for clarity.

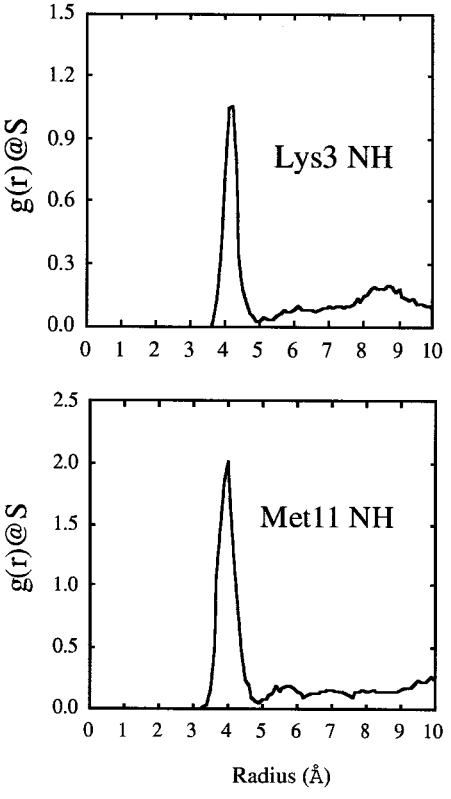

FIGURE 9 RDFs of amide nitrogen of peptide backbone residues Lys-3 and Met-11 with the sulfur atom of the lipid headgroup. The large first peak in the RDF at a distance of 4.1 Å signifies hydrogen bonding between amide hydrogen and the sulfate oxygen atoms.

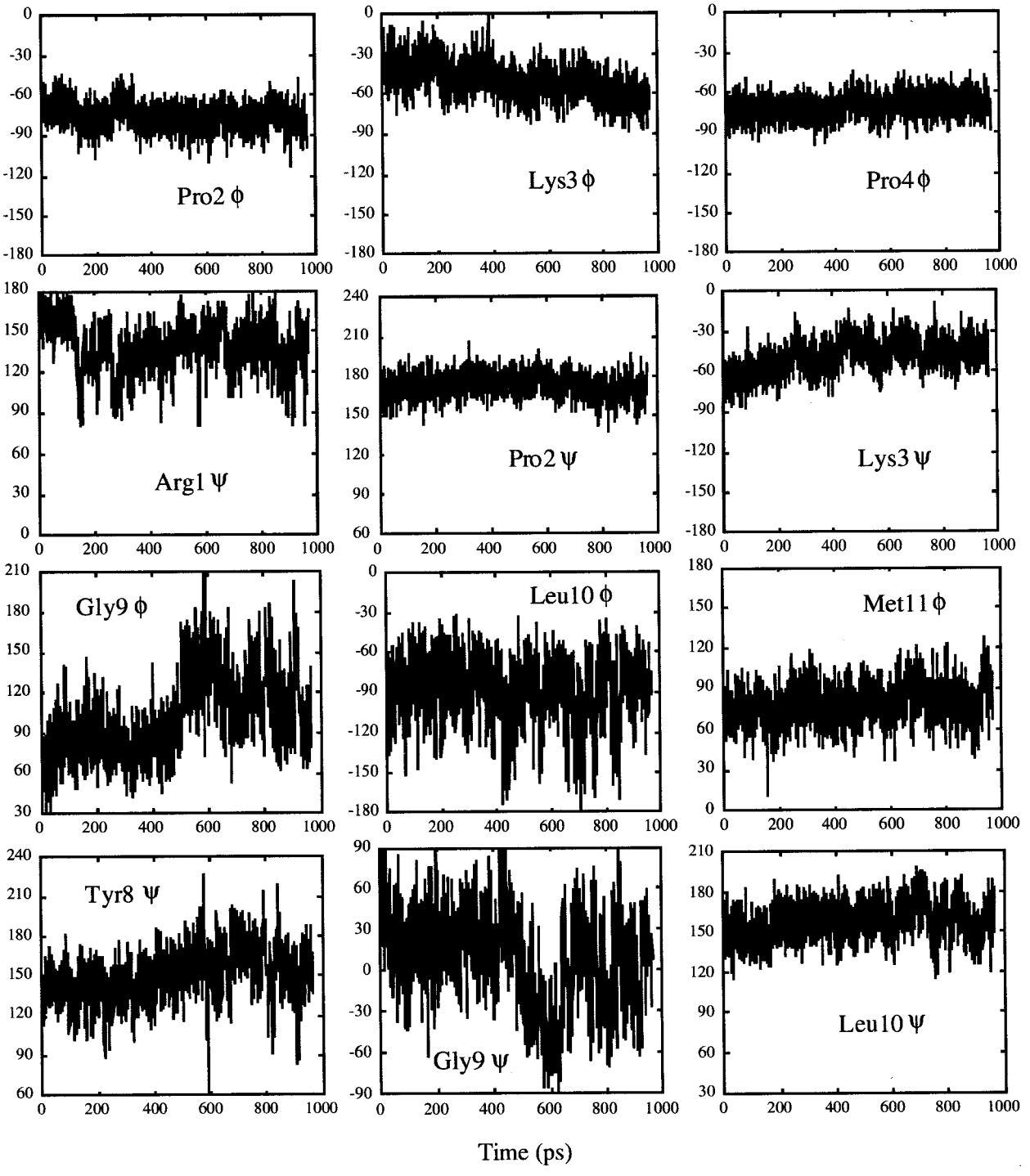

FIGURE 10 The time series for ϕ-ψ dihedral angles of SP-Y8 in an SDS micelle. *Top two rows:* the time series for the ϕ-ψ dihedral angles for the three N-terminal residues. *Bottom two rows:* the time series for the ϕ-ψ dihedral angles for the three C-terminal residues.

proteins, but not as flexible as random coil. The results on alamethicin in SDS micelles also showed that even though the peptide has secondary structure characteristics, the peptide still experiences large fluctuations about the average conformation. This fact should be kept in mind when trying to make such fine distinctions in the secondary structure of small peptides, e.g., between different categories of helices and consecutive type I β-turns.

DISCUSSION AND CONCLUSIONS

SP peptides in SDS micelle

Comparison of the simulations of SP and SP-Y8 in the SDS micelle shows similar gross positional and orientational properties. The section that is most different between the two peptides in the biphasic cell simulations is that of Arg-1 through Gln-6. However, this section of both peptides ap-

pears very similar in the orientation of the backbone and position of the side chains in SDS micelles. Both showed similar properties with regard to electrostatic interaction with the headgroups, which forces this section of SP-Y8 to be in the interfacial area. The side chain of Lys-3 seems to play a large part in positioning of the peptide at the interface. Interestingly, this configuration was not part of the initial configuration but developed over the equilibration period of the simulation. SP and SP-Y8 differ the most in the orientations of the two aromatic side chains. SP-Y8 has the two aromatic side chains on opposite faces with Phe-7 in contact with the methylenes of the hydrocarbon chain of SDS and Tyr-8 well solvated by water. SP has both phenylalanines in contact with the hydrocarbon chains or in the headgroup region. Furthermore, the faces of the aromatic side chains in SP are in close contact, giving rise to favorable van der Waals (vdw) interactions (or aromatic stacking) between them. These favorable vdw interactions between the two aromatic side chains are not seen in SP-Y8 for either the biphasic cell or micelle simulations. Because of such a difference in the orientation of the backbone and the position of the side chains between the two peptides we would expect a difference in the hydrophobic interactions and thus in the ΔG_{part} between the two peptides upon partitioning in the SDS micelle. The experimental value of 0.35 kcal/mol for the difference in ΔG_{part} for these two peptides in DPC micelles (more negative for SP) (Wong and Gao, 1998) is in agreement with this observation. Recent work on the conformation of SP, its agonists, and antagonists provided speculations on the significance of the relative orientations of the two aromatic rings to provide aromatic-aromatic stacking interactions for binding and receptor recognition and activation (Desai et al., 1992; Huang et al., 1994; Josien et al., 1994; Grdadolnik et al., 1994). It is thus interesting to note that the relative orientations of the two aromatic rings for SP and SP-Y8 are different when these two peptides are placed at the water-membrane interface. The reduction in the potency of SP-Y8 as compared to SP (Fisher et al., 1976) may be a result of the partial loss of the π-π interaction between the two aromatic rings (in residues 7 and 8) in SP-Y8 when it is bound to the membrane. However, it is also conceivable that the lower potency may be a direct result of the lower affinity of SP-Y8 for the membrane (Wong and Gao, 1998), if the membrane-mediated mechanism for receptor binding as proposed by Schwyzer is valid for these SP peptides (Schwyzer, 1992).

The simulations of SP peptides in an explicit SDS micelle have allowed for the classification of a diverse range of peptide-lipid interactions. The orientation of the peptide parallel to the interface is due to the polarity of the peptide backbone in that the peptide backbone should be solvated by water or be intramolecularly hydrogen-bonded. The interaction of the peptide with the micelle is mainly through the hydrophobic interaction of the side chains of Pro-4, Phe-7, Leu-10, Met-11, and Phe-8. In addition, the N-terminal amino hydrogen atoms, the Arg-1 side chain, Lys-3 N-H and N_ζ hydrogen atoms, and Met-11 NH have significant electrostatic and/or hydrogen bonding interactions with the SDS headgroups. Even if SP forms an α-helix, this conformation still leaves the final residues without intramolecular hydrogen bonds, which would be thermodynamically unstable if inserted into the micellar core (Ben-Tal et al., 1996, 1997). Despite the distinct charged and hydrophobic segments (primary amphiphilicity as defined by Schwyzer) of these peptides, Schwyzer's model for the membrane-bound state of SP of insertion of the hydrophobic segment (Schwyzer, 1992, 1995) seems unlikely. One of Duplaa's models (1992) for the membrane-bound state of SP, in which both phenylalanine residues are embedded into the membrane, agrees with our simulations of SP.

The results of Kothekar's (1996) MD simulation of SP in a phospholipid bilayer for 260 ps using the insertion model as the initial configuration are suspect. The results of this work show that it requires much more than 260 ps for the peptide to equilibrate to the optimized orientation/position with respect to the water/membrane interface. Not surprisingly, the results of Kothekar's work showed that SP was in an insertion mode in the bilayer that was basically the same as the initial configuration.

This work is the first MD simulation of a peptide in a micelle that is most frequently used in high resolution NMR, and it provides simulation results for direct comparison with and interpretation of experimental results for the same systems. Our three-dimensional models of the SP/SP-Y8-micelle complex could serve as a good starting point for assessing the importance of particular residues to membrane binding and how membrane binding is related to activation of the NK1 receptor (Seelig et al., 1996). With the increasing use of supercomputers and parallel algorithm development, nanosecond simulations of peptide-membrane complexes will become more routine. Our simulations were broken up into 80-ps sections that required ~420 cpu hours on a Cray T3E at the Pittsburgh Supercomputing Center for each section. Using 32 processors allows each of these sections to be calculated in ~13 h assuming that 1 cpu hour is equal to 1 h wall time.

There are concerns that in the *NVT* simulation the constant volume may prevent the system from evolving to an incorrect density despite producing apparently good but spurious results. This could happen if the force field was flawed (Jakobbsen et al., 1996). The CHARMM parameters have been tested in a number of examples (MacKerell et al., 1998; MacKerell, 1995; Feller et al., 1997) and have shown excellent results. Recent results suggest that some form of constant pressure or constant surface tension is the most appropriate way to simulate interfacial systems (Chiu et al., 1995; Feller et al., 1995; Tu et al., 1996) and future studies will be carried out in such an ensemble. Studies are also currently underway to quantitatively define the dynamics of the lipids and the peptide in the form of time correlation functions and to compare with NMR relaxation data.

Comparison of simulations in the biphasic cell versus an explicit SDS micelle

Certainly, constructing an environment that has properties of not only both hydrophilic and hydrophobic environments but also an interfacial region will be useful in refining structures taken from SA treatments in vacuum (Chiche et al., 1989). A more complete picture of the properties of peptides and other amphipathic molecules at hydrophilic/hydrophobic interfaces is vitally important to the membrane-bound state of such molecules. The use of the biphasic cell in constructing models for the peptide-micelle complex has been shown to reproduce many of the experimental properties of such a system, and reveal some detailed structural and dynamic properties of the peptides that are not easily accessible experimentally (see preceding paper; Guba and Kessler, 1994; Guba et al., 1994). Yet water/hydrophobic interfaces are clearly not the same as micelles or lipid bilayers in that usually the interface is more distinct. Weiner and White (1992) have shown the interface of lipid bilayers to be quite heterogeneous and broad. Furthermore, the water/hydrophobic interface neglects the often very important electrostatic interactions played by the headgroups. As a result of this work on SP peptides in an explicit SDS micelle and the results from the preceding paper on the same peptides in the biphasic system, we can make a more definite comparison between the two systems and comment on the merits of the biphasic system as an approximation for a more realistic explicit water/membrane mimicking system. Overall, the results seem to indicate that if the peptide has a significant hydrophobic interaction with the micelle, the biphasic cell can reproduce most of the properties of the peptide-micelle complex. If, in addition, the peptide has significant electrostatic interactions with the headgroup or contains interfacial lysines that may interact both with the methylenes and the charged headgroup of the lipids, then the biphasic cell may give incomplete or misleading results on both the structure and the dynamics of the segment(s) of the peptide having electrostatic interactions with the micelle. The present results also showed that the simulations done in the biphasic cell may have exaggerated the differences between SP and SP-Y8 due to the absence of a broad heterogeneous interfacial area. For example, a hydrophobic side chain that is inserted into the micellar core may be substituted for a more polar side chain that hydrogen-bonds to the headgroup. Both of these peptides may still retain similar orientations at the micellar surface, but simulations in the biphasic cell would likely show the two side chains in completely different environments (water versus carbon tetrachloride), which may in turn cause the orientation of the whole peptide to differ, as observed in the 1-6 segment of these two peptides in the biphasic simulation.

However, the important conclusion that can be drawn from the comparison of the results between the simulations in these two systems is that the simulation in the biphasic cell can reproduce the gross orientational and positional properties of the peptide-micelles system (and presumably peptide-bilayer systems as well). The distribution of the backbones and side chains in respective phases and hydrogen-bonding characteristics are also qualitatively similar in these simulations. Since the biphasic system contains only about one-third of the number of atoms of the peptide-micelles system, and we have demonstrated in this study that the equilibration time for peptide in the former system is ~200 ps vs. 450–500 ps for the latter, it is conceivable that one could use the equilibration in the biphasic system to obtain the proper starting configuration for the peptide (with respect to the water-membrane interface) in about one-fifth of the equilibration time required for the real peptide-micelle or peptide-bilayer system before starting to sample the dynamic trajectories for the real system of interest.

We thank Dr. Alexander MacKerell for providing the coordinates of the equilibrated SDS micelle, and gratefully acknowledge the support of Dr. Hossein Tahani and the University of Missouri Campus Computing.

This work was supported by Grant MCB950034P from the Pittsburgh Supercomputing Center, sponsored by the National Science Foundation (NSF), and by a grant from the Research Council of the University of Missouri, Columbia.

REFERENCES

Attwood, D., and A. T. Florence. 1983. *In* Surfactant Systems. Chapman and Hall, New York. 71.

Belohorcova, K., J. H. Davis, T. B. Woolf, and B. Roux. 1997. Structure and dynamics of an amphiphilic peptide in a lipid bilayer: a molecular dynamics study. *Biophys. J.* 73:3039–3055.

Ben-Tal, N., A. Ben-Shaul, A. Nicholls, and B. Honig. 1996. Free-energy determinants of α-helix insertion into lipid bilayers. *Biophys. J.* 70: 1803–1812.

Ben-Tal, N., D. Sitkoff, I. Topol, A. Yang, S. Burt, and B. Honig. 1997. Free energy of amide hydrogen bond formation in vacuum, in water, and in liquid alkane solution. *J. Phys. Chem. B.* 101:450–457.

Brooks, B. R., R. E. Bruccoleri, B. D. Olafson, D. J. States, S. Swaminathan, and M. Karplus. 1983. CHARMM: a program for macromolecular energy, minimization, and dynamics calculations. *J. Comp. Chem.* 4:187–217.

Brown, J., and W. Huestis. 1993. Structure and orientation of a bilayer-bound model tripeptide. A ^{1}H-NMR study. *J. Phys. Chem.* 97: 2967–2973.

Chiche, L., C. Gaboriaud, A. Heitz, J.-P. Mornon, B. Castro, and P. Kollman. 1989. Use of restrained molecular dynamics in water to determine three-dimensional protein structure: prediction of the three-dimensional structure of ecballium elaterium trypsin inhibitor II. *Proteins: Struct., Funct., Genet.* 6:405–417.

Chiu, S.-W., M. Clark, V. Balaji, S. Subramaniam, H. L. Scott, and E. Jakobsson. 1995. Incorporation of surface tension into molecular dynamics simulation of an interface: a fluid phase lipid bilayer membrane. *Biophys. J.* 69:1230–1245.

Convert, O., H. Duplaa, S. Lavielle, and G. Chassaing. 1991. Influence of the replacement of amino acid by its D-enantiomer in the sequence of substance P. 2. Conformational analysis by nmr and energy calculations. *Neuropeptides*. 19:259–270.

Croonen, Y., E. Gelade, M. Van der Ziegel, H. Van der Auweraer, F. C. Vandendriessche, and F. C. DeSchryver. 1983. Influence of salt, detergent concentration, and temperature on the fluorescence quenching of 1-methylpyrene in sodium dodecylsulfate with m-dichlorobenzene. *J. Phys. Chem.* 87:1426.

Damodaran, K. V., and K. M. Merz. 1995. Interaction of the fusion inhibiting peptide carbobenzoxy-D-Phe-L-Phe-Gly with N-methyldioleoylphosphatidylethanolamine lipid bilayers. *J. Am. Chem. Soc.* 117: 6561–6571.

Damodaran, K. V., K. M. Merz, and B. P. Gaber. 1995. Interaction of small peptides with lipid bilayers. *Biophys. J.* 69:1299–1308.

Desai, V. C., S. L. Lefkowitz, P. F. Thadeio, K. P. Longo, and R. M. Snider. 1992. Discovery of a potent substance P antagonist: recognition of the key molecular determinant. *J. Med. Chem.* 35:4911–4913.

Duplaa, H., O. Convert, A.-M. Sautereau, J.-F. Tocanne, and G. Chassaing. 1992. Binding of substance P to monolayers and vesicles made of phosphatidylcholine and/or phosphatidylserine. *Biochim. Biophys. Acta.* 1107:12–22.

Feller, S. E., D. Yin, R. W. Pastor, and A. D. MacKerell, Jr. 1997. Molecular dynamics simulation of unsaturated lipid bilayers at low hydration: parametrization and comparison with diffraction studies. *Biophys. J.* 73:2269–2279.

Feller, S. E., Y. Zhang, R. W. Pastor, and B. R. Brooks. 1995. Constant pressure molecular dynamics simulation: the Langevin piston method. *J. Chem. Phys.* 103:4613–4621.

Fisher, G., K. Folkers, B. Pernow, and C. Bowers. 1976. Synthesis and some biological activities of the tyrosine-8 analog of substance P. *J. Med. Chem.* 19:325–328.

Frey, S., and L. K. Tamm. 1991. Orientation of melittin in phospholipid bilayers: a polarized attenuated total reflection infrared study. *Biophys. J.* 60:922–930.

Gennis, R. B. 1989. Biomembranes: Molecular Structure and Function. Springer-Verlag, New York.

Grdadolnik, S. G., D. F. Mierke, G. Byk, I. Zeltser, C. Gilon, and H. Kessler, 1994. Comparison of the conformation of active and nonactive backbone cyclic analogs of substance P as a tool to elucidate features of the bioactive conformation: NMR and molecular dynamics in DMSO and water. *J. Med. Chem.* 37:2145–2152.

Guba, W., R. Haessner, G. Breipohl, S. Henke, J. Knolle, V. Santagada, and H. Kessler. 1994. Combined approach of NMR and molecular dynamics within a biphasic membrane mimetic. Conformation and orientation of the bradykinin antagonist Hoe. 140. *J. Am. Chem. Soc.* 116:7532–7540.

Guba, W., and H. Kessler. 1994. A novel computational mimetic of biological membranes in molecular dynamics simulations. *J. Phys. Chem.* 98:23–27.

Huang, P., and G. H. Loew. 1995. Interaction of an amphiphilic peptide with a phospho-lipid bilayer surface by molecular dynamics simulation study. *J. Biomol. Struct. Dyn.* 12:937–956.

Huang, R. R. C., H. Yu, C. Strader, and T. M. Fong. 1994. Interaction of substance P with the second and seventh transmembrane domains of the neurokinin-1 receptor. *Biochemistry*. 33:3007–3013.

Itri, R., and L. Q. Amaral. 1991. Distance distribution function of sodium dodecylsulfate micelles by x-ray scattering. *J. Phys. Chem.* 95:423–427.

Jacobs, R., and S. H. White. 1989. The nature of the hydrophobic binding of small peptides at the bilayer interface: implications for the insertion of transbilayer helices. *Biochemistry*. 28:3421–3437.

Jakobbsen, E., S. Subramaniam, and H. L. Scott. 1996. Strategic issues in molecular dynamics simulations of membranes. *In* Biological Membranes: A Molecular Perspective from Computation and Experiment. K. M. Merz, Jr., and B. Roux, editors. Birkhäuser, Boston. 105–123.

Jorgenson, W. L., R. W. Impey, J. Chandrasekhar, J. D. Madura, and M. L. Klein. 1983. Comparison of simple potential functions for simulating liquid water. *J. Chem. Phys.* 79:926–935.

Josien, H., S. Lavielle, A. Brunissen, M. Saffroy, Y. Torrens, J.-C. Beaujouan, J. Glowinski, and G. Chassaing, 1994. Design and synthesis of side-chain conformationally restricted phenylalanines and their use for structure-activity studies on tachykinin NK-1 receptor. *J. Med. Chem.* 37:1586–1601.

Keire, D., and T. Fletcher. 1996. The conformation of substance P in lipid environments. *Biophys. J.* 70:1716–1727.

Kothekar, V. 1996. 260 ps molecular dynamics simulation of substance P with hydrated dimyristoylphosphatidyl choline bilayer. *J. Biomol. Struct. Dyn.* 13:601–613.

MacKerell, Jr., A. D. 1995. Molecular dynamics simulation analysis of a sodium dodecyl sulfate micelle in aqueous solution: decreased fluidity of the micelle hydrocarbon interior. *J. Phys. Chem.* 99:1846–1855.

MacKerell, Jr., A. D., D. Bashford, M. Bellott, R. L. Dunbrack, Jr., J. D. Evanseck, M. J. Field, S. Fischer, J. Gao, H. Guo, S. Ha, D. Joseph-McCarthy, L. Kuchnir, K. Kuczera, F. T. K. Lau, C. Mattos, S. Michnick, T. Ngo, D. T. Nguyen, B. Prodhom, W. E. Reiher III, B. Roux, M. Schlenkrich, J. C. Smith, R. Stote, J. Straub, M. Watanabe, J. Wiorkiewicz-Kuczera, D. Yin, and M. Karplus. 1998. All-atom empirical potential for molecular modeling and dynamics studies of proteins. *J. Phys. Chem. B*. 102:3586–3616.

Merz, Jr., K. M., and B. Roux, editors. 1996. Biological Membranes: A Molecular Perspective from Computation and Experiment. Birkhäuser, Boston.

Oda, K., H. Miyagawa, and K. Kitamura. 1996. How does the electrostatic force cut-off generate non-uniform temperature distributions in proteins? *Mol. Sim.* 16:167–177.

Opella, S. J. 1997. NMR and Membrane Proteins. *Nat. Struct. Biol., NMR Suppl*. 845–848.

Ravishanker, G., S. Vijakumar, and D. L. Beveridge. 1994. STRIPS: An algorithm for generating two-dimensional hydrogen-bond topology diagrams for proteins. *In* Modeling the Hydrogen Bond. The American Chemical Society, Washington, DC. 209–219.

Roseman, M. A. 1988. Hydrophobicity of the peptide C=O–H-N hydrogen bonded group. *J. Mol. Biol.* 201:621–625.

Roux, B., and T. B. Woolf. 1996. Molecular dynamics of Pf1 coat protein in a phospholipid bilayer. *In* Biological Membranes: A Molecular Perspective from Computation and Experiment. K. M. Merz, Jr., and B. Roux, editors. Birkhäuser, Boston. 555–587.

Ryckaert, J.-P., G. Cicotti, and H. J. C. Berendsen. 1977. Numerical integration of the Cartesian equations of motion of a system with constraints: molecular dynamics of n-alkanes. *J. Comput. Phys.* 23: 327–341.

Sanders, C. R., and G. C. Landis. 1995. Reconstitution of membrane proteins into lipid-rich bilayered mixed micelles for nmr studies. *Biochemistry*. 43:4030–4040.

Schlenkrich, M., J. Brickmann, A. D. MacKerell, Jr., and M. Karplus. 1996. An empirical potential energy function for phospholipids: criteria for parameter optimization and applications. *In* Biological Membranes: A Molecular Perspective from Computation and Experiment. K. M. Merz and B. Roux, editors. Birkhäuser, Boston.

Schwyzer, R. 1992. Conformations and orientations of amphiphilic peptides induced by artificial lipid membranes: correlations with biological activity. *Chemtracts–Biochem. and Mol. Biol.* 3:347–379.

Schwyzer, R. 1995. 100-Year lock-and-key concept: are peptide keys shaped and guided to their receptors by the target cell membrane? *Biopolymers*. 37:5–16.

Seelig, A., T. Alt, S. Lotz, and G. Hölzemann. 1996. Binding of substance P agonists to lipid membranes and to the neurokinin-1 receptor. *Biochemistry*. 35:4365–4374.

Seelig, A., and P. M. Macdonald. 1989. Binding of a neuropeptide, substance P, to neutral and negatively charged lipids. *Biochemistry*. 28: 2490–2496.

Segrest, J. P., H. De Loof, J. G. Dohlmann, C. G. Brouillette, and G. M. Anantharamaiah. 1990. Amphipathic helix motif: classes and properties. *Proteins: Struct., Funct., Genet.* 8:103–117.

Shen, L., D. Bassolino, and T. Stouch. 1997. Transmembrane helix structure, dynamics, and interactions: multi-nanosecond molecular dynamics simulations. *Biophys. J.* 73:3–20.

Soderman, O., G. Carlstrom, U. Olsson, and T. C. Wong. 1988. NMR relaxation in micelles. ^{2}H relaxation at three field strengths of three positions on the alkyl chain of sodium dodecyl sulfate. *J. Chem. Soc. Faraday Trans. 1*. 84:4475–4486.

Spyracopoulos, L., A. A. Yee, and J. D. J. O'Neil. 1996. Backbone dynamics of an alamethicin in methanol and aqueous detergent solution determined by heteronuclear ^{1}H-^{15}N NMR spectroscopy. *J. Biomol. NMR*. 7:283–294.

Steinbach, P., and B. R. Brooks. 1994. New spherical-cutoff methods for long range forces in macromolecular simulation. *J. Comp. Chem.* 15: 667–683.

Tu, K., D. J. Tobias, J. K. Blasie, and M. L. Klein. 1996. Molecular dynamics investigation of the structure of a fully hydrated gel-phase dipalmitoylphosphatidylcholine bilayer. *Biophys. J.* 70:595–608.

Weiner, M. C., and S. H. White. 1992. Structure of a fluid dioleoylphosphatidylcholine bilayer determined by joint refinement of x-ray and neutron diffraction data. III. Complete structure. *Biophys J.* 61: 434–447.

White, S., and W. C. Wimley. 1994. Peptides in lipid bilayers: structural and thermodynamic basis for partitioning and folding. *Curr. Opin. Struct. Biol.* 4:79–86.

Williams, R. W., and J. L. Weaver. 1990. Secondary structure of substance P bound to liposomes in organic solvents and in solution from Raman and CD spectroscopy. *J. Biol. Chem.* 265:2505–2513.

Wilmot, C. M., and J. M. Thorton. 1990. β-Turns and their distortions: a proposed new nomenclature. *Protein Eng.* 3:479–493.

Wimley, W. C., and S. H. White. 1996. Experimentally determined hydrophobicity scale for proteins at membrane interfaces. *Nat. Struct. Biol.* 3:842–848.

Wong, T. C., and X. Gao. 1998. The temperature dependence and thermodynamic functions of partitioning of substance P peptides in dodecylphosphocholine micelles. *Biopolymers*. 45:395–403.

Woolf, T. B. 1998. Molecular-dynamics simulations of individual α-helices of bacteriorhodopsin in dimyristoylphosphatidylcholine. II. Interaction energy analysis. *Biophys. J.* 74:115–131.

Woolf, T. B., A. Grossfield, K. MacKenzie, and D. Engelman. 1998. Helix:lipid interactions in glycophorin dimerization: molecular dynamics calculations. *Biophys. J.* 74:A15.

Woolf, T. B. and B. Roux. 1996. Structure, energetic, and dynamics of lipid-protein interactions: a molecular dynamics study of the gramicidin A channel in a DMPC bilayer. *Proteins: Struct., Funct., Genet.* 24:92–114.

Woolley, G. A., and C. M. Deber. 1987. Peptides in membranes: lipid-induced secondary structure of substance P. *Biopolymers*. 26: S109–S121.

Young, J. K., C. Anklin, and R. P. Hicks. 1994. NMR and molecular modeling investigations of the neuropeptide substance P in the presence of 15 mM sodium dodecyl sulfate micelles. *Biopolymers*. 34:1449–1462.

Zhou, F., and K. Schulten. 1996. Molecular dynamics study of phospholipase A_2 on a membrane surface. *Proteins: Struct., Funct., Genet.* 25:12–27.